

THREE-PORT FULL-BRIDGE CONVERTERS WITH WIDE VOLTAGE RANGE INPUT FOR SOLAR POWER SYSTEMS

M.Ragavendran¹, Dr. M. Sasikumar²,

1PG Scholars, Dept. of Power Electronics and Drives, Jeppiaar Engineering College, Chennai.

ragavanworld@gmail.com

2Professor & Head, Dept. of Power Electronics and Drives, Jeppiaar Engineering College, Chennai.

pmsasi77@yahoo.co.in

Abstract— A systematic method for deriving three-port converters (TPCs) from the full-bridge converter (FBC) is proposed in this paper. The proposed method splits the two switching legs of the FBC into two switching cells with different sources and allows a dc bias current in the transformer. By using this systematic method, a novel full-bridge TPC (FB-FBC) is developed for renewable power system applications which feature simple topologies and control, a reduced number of devices, and single-stage power conversion between any two of the three ports. The proposed FB-TPC consists of two bidirectional ports and an isolated output port. The primary circuit of the converter functions as a buck-boost converter and provides a power flow path between the ports on the primary side. The FB-TPC can adapt to a wide source voltage range, and tight control over two of the three ports can be achieved while the third port provides the power balance in the system. Furthermore, the energy stored in the leakage inductance of the transformer is utilized to achieve zero-voltage switching for all the primary-side switches. The FB-TPC is analyzed in detail with operational principles, design considerations, and a pulse-width modulation scheme (PWM), which aims to decrease the dc bias of the transformer.

Experimental results verify the feasibility and effectiveness of the developed FB-TPC. The topology generation concept is further extended, and some novel TPCs, dual-input, and multiport converters are presented.

Index Terms—Boost-buck, dc-dc converter, full-bridge converter (FBC), Solar power system, three-port converter (TPC).

I. INTRODUCTION

Solar power systems, which are capable of harvesting energy from solar cells, fuel cells are found in many applications such as hybrid electric vehicles, satellites, traffic lights, and powering remote communication systems.

Since the output power of renewable sources is stochastic and the sources lack energy storage capabilities, energy storage systems such as a battery or a super capacitor are required to improve the system dynamics and steady-state characteristics. A three-port converter (TPC), which can interface with solar sources, storage elements, and loads, simultaneously, is a good candidate for a renewable power system and has recently attracted increased research interest. Compared with the conventional solutions that employ multiple converters, the TPC features single-stage conversion between any two of the three ports, higher system efficiency, fewer components, faster response, compact packaging,

and unified power management among the ports with centralized control. As a result of these remarkable merits, many TPCs have been proposed recently for a variety of applications. One way to construct a TPC is to interface several conversion stages to a common dc bus. But this is not an integrated solution since only a few devices are shared. Power flow control and zero-voltage switching (ZVS) are achieved with phase-shift control between different switching bridges,

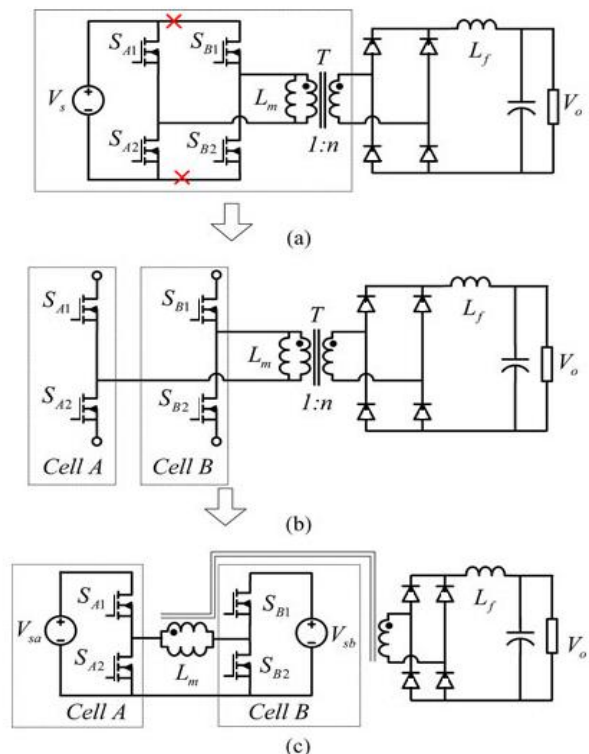


Fig. 1. Proposed derivation of full-bridge three-port converter. (a) Full-bridge Converter. (b) Two-switching cells. (c) Three-port Full-bridge converter.

Full-bridge TPC (FB-TPC) with single-stage power conversion between any two of the three ports. Furthermore, from a topological point of view, because a buck-boost converter is integrated in the proposed FB-TPC, it can adapt to applications with a wide source voltage range. ZVS of all the primary-side switches can also be achieved with the proposed-TPC. This paper is organized as follows. In Section II, the basic ideas used to generate FB-TPC are proposed. In Section-III, the FB-TPC is analyzed in detail, with operation principles, design considerations, and modulation methods given to verify the proposed method. Experimental results are presented in Section IV.

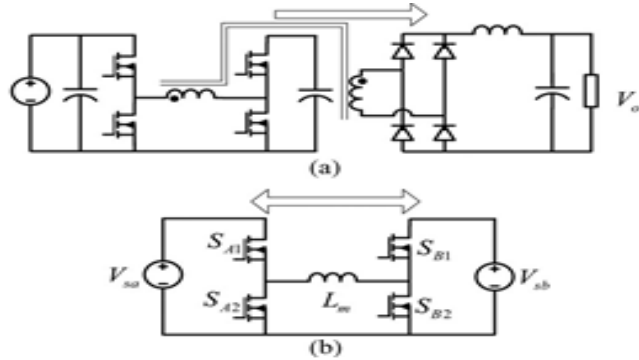


Fig. 2. Equivalent circuits. (a) Between source and load. (b) Between the two sources.

The topology generation method of the FB-TPC is further extended in Section V. Finally, conclusions will be given in Section VI.

II. DERIVATION OF THE FB-TPC FROM A FULL-BRIDGED DC-DC CONVERTER

Referring to Fig. 1(a), the primary side of the FBC consists of two switching legs, composed of S_{A1}, S_{A2} and S_{B1}, S_{B2} , in parallel, connected to a common input source V_s . For the primary side of the FBC, the constraint condition of the operation of the FBC is the voltage-second balance principle of the magnetizing inductor L_m . This means that, from a topological point of view, the two switching legs of the FBC can also be split into two symmetrical parts, cells A and B, if only L_m satisfies the voltage-second balance principle, as shown in Fig. 1(b). The two cells can be connected to different sources, V_{sa} and V_{sb} , respectively, as shown in Fig. 1(c), and then a novel FB-TPC is derived. The voltage of the two sources of the FB-TPC can be arbitrary. Specially, if V_{sa} always equals V_{sb} , the two cells can be paralleled directly and then the conventional FBC is derived.

Therefore, the FBC can be seen as a special case of the FB-TPC as shown in Fig. 1(c). Close observation indicates that the FB-TPC has a symmetrical structure and both V_{sa} and V_{sb} can supply power to the load V_o . The equivalent circuit from one of the source ports to the load port is shown in Fig. 2(a). In addition, a bidirectional buck-boost converter is also integrated in the primary side of the FB-TPC by employing the magnetizing inductor of the transformer L_m as a filter inductor. With the bidirectional buck-boost converter, the power flow paths between the two sources, V_{sa} and V_{sb} , can be configured and the power can be transferred between V_{sa} and V_{sb} freely. The equivalent circuit between the two sources is illustrated in Fig. 2(b). According to the equivalent circuits shown in Fig. 2, it can be seen that the power flow paths between any two of the three ports, V_{sa}, V_{sb} , and V_o , have been

built. The unique characteristics of the FB-TPC are analyzed and summarized as follows.

1) The FB-TPC has two bidirectional ports and one isolated output port. Single-stage power conversion between any two of the three ports is achieved. The FB-TPC is suitable for renewable power systems and can be connected with an input source and an energy storage element, such as the photovoltaic (PV) with a battery backup, or with two energy storage elements, such as the hybrid battery and the super capacitor power system.

2) A buck-boost converter is integrated in the primary side of the FB-TPC. With the integrated converter, the source voltage V_{sa} can be either higher or lower than V_{sb} , and vice versa. This indicates that the converter allows the sources' voltage varies over a wide range.

3) The devices of the FB-TPC are the same as the FBC and no additional devices are introduced which means high integration is achieved.

4) The following analysis will indicate that all four active switches in the primary side of the FB-TPC can be operated with ZVS by utilizing the energy stored in the leakage inductor of the transformer, whose principle is similar to the phase-shift FBC.

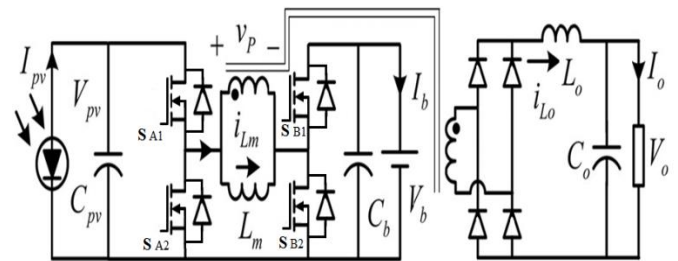


Fig. 3. Topology of the proposed FB-TPC.

III. ANALYSIS OF THE FB-TPC FOR THE STAND-ALONE SOLAR POWER SYSTEM APPLICATION

The FB-TPC, as shown in Fig. 1(b), is applied to a stand-alone PV power system with battery backup to verify the proposed topology. To better analyze the operation principle, the proposed FB-TPC topology is redrawn in Fig. 3, the two source ports are connected to a PV source and a battery, respectively, while the output port is connected to a load. There are three power flows in the standalone PV power system: 1) from PV to load; 2) from PV to battery; and 3) from battery to load. As for the FB-TPC, the load port usually has to be tightly regulated to meet the load requirements, while the input port from the PV source should implement the maximum power tracking to harvest the most energy. Therefore, the mismatch in power between the PV source and load has to be charged into or discharged from the battery port, which means that in the FB-TPC, two of the three ports should be controlled independently and the third one used for power balance. As a result, two independently controlled variables are necessary.

A. Switching State Analysis

Ignoring the power loss in the conversion, we have

$$p_{pv} = p_b + p_o(1)$$

Where p_{pv} , p_b , and p_o are the power flows through the PV, battery, and load port, respectively. The FB-TPC has three possible operation modes:

1) dual-output (DO) mode, with $p_{pv} \geq p_o$, the battery absorbs the surplus solar power and both the load and battery take the power from PV;

(2) dual-input (DI) mode, with $p_{pv} \leq p_o$ and $p_{pv} > 0$, the battery discharges to feed the load along with the PV;

(3) single-input single-output (SISO) mode, with $p_{pv} = 0$, the battery supplies the load power alone.

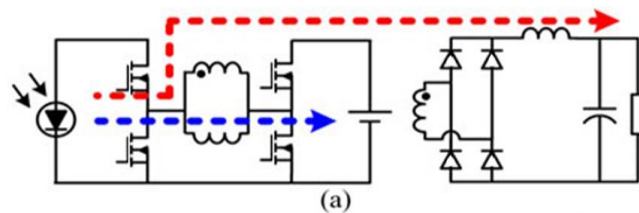
When $p_{pv} = p_o$ exactly, the solar supplies the load power alone and the converter operates in a boundary state of DI and DO modes. This state can either be treated as DI or DO mode. Since the FB-TPC has a symmetrical structure, the operation of the converter in this state is the same as that of SISO mode, where the battery feeds the load alone. The operation modes and power flows of the converter are listed in Table I. The power flow paths/directions of each operation mode have been illustrated in Fig. 4. The switching states in different operation modes are the same and the difference between these modes are the value and direction of i_{Lm} , as shown in Fig. 3, which is dependent on the power of p_{pv} and p_o . In the DO mode, i_{Lm} is positive, in the SISO mode, i_{Lm} is negative, and in the DI mode, i_{Lm} can either

TABLE-I-OPERATION MODES OF THE FB-TPC

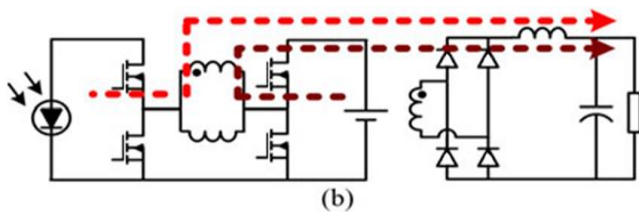
Operation modes	Power of PV	Power of battery
Dual-output mode	$p_{pv} \geq p_o$	Battery charging, $p_b \geq 0$
Dual-input mode	$p_{pv} \leq p_o, p_{pv} > 0$	Battery discharging, $p_b < 0$
Single-input single-output mode	$p_{pv} = 0$	Battery discharging, $p_b = -p_o$

MODES OF OPERATION

MODE: 1



MODE: 2



MODE: 3

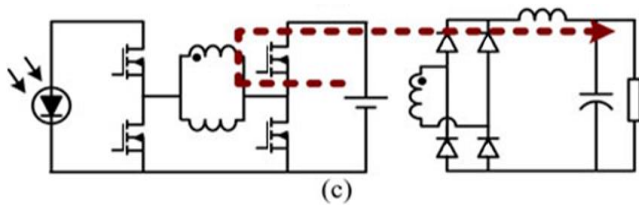


Fig. 4. Power flow paths/directions of each operation mode. (a) DO mode. (b) DI mode. (c) SISO mode.

be positive or negative. Take the DO mode as an example to analyze.

For simplicity, the following assumptions are made

- 1) C_{pv}, C_b , and C_o are large enough and the voltages of the three ports, V_{pv} , V_b , and V_o , are constant during the steady state; and
- 2) the $V_{pv} \geq V_b$ case is taken as an example for the switching state analysis.

There are four switching states in one switching cycle. The key waveforms and the equivalent circuit in each state are shown in Figs. 5 and 6, respectively.

State I [t0 -t1]: Before t_0 , S_{A2} and S_{B2} are ON and S_{A1} and S_{B1} are OFF, while i_{Lm} freewheels through S_{A2} and S_{B2} . At t_0 , S_{A1} turns ON and S_{A2} turns OFF. A positive voltage is applied across the transformer's primary winding [see Fig. 6(a)]

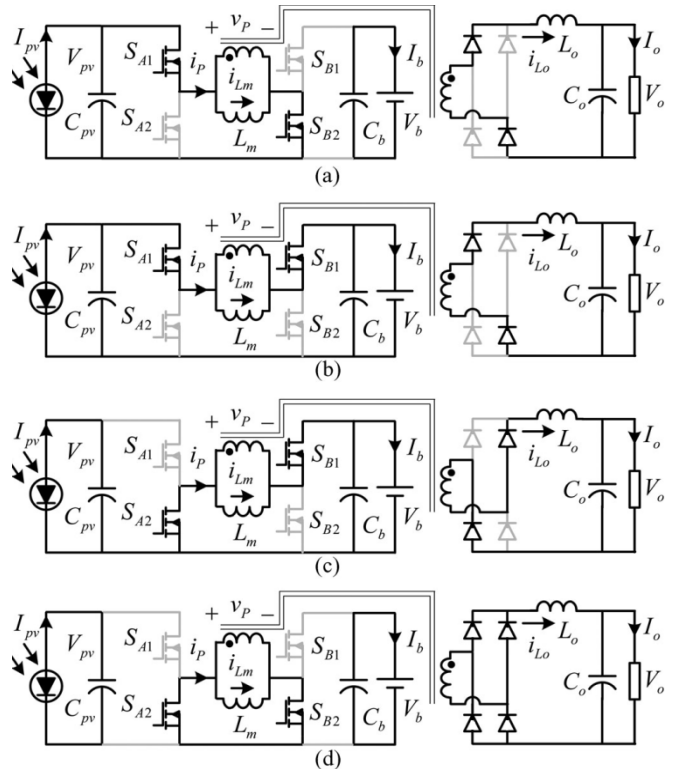


Fig. 5. Equivalent circuits of each switching state. (a) [t0, t1]. (b) [t1, t2]. (c) [t2, t3]. (d) [t3, t4].

State II [t1 -t2]: At t_1 , S_{B2} turns OFF and S_{B1} turns ON. A positive voltage is applied on the primary winding of the transformer [see Fig. 6(b)]

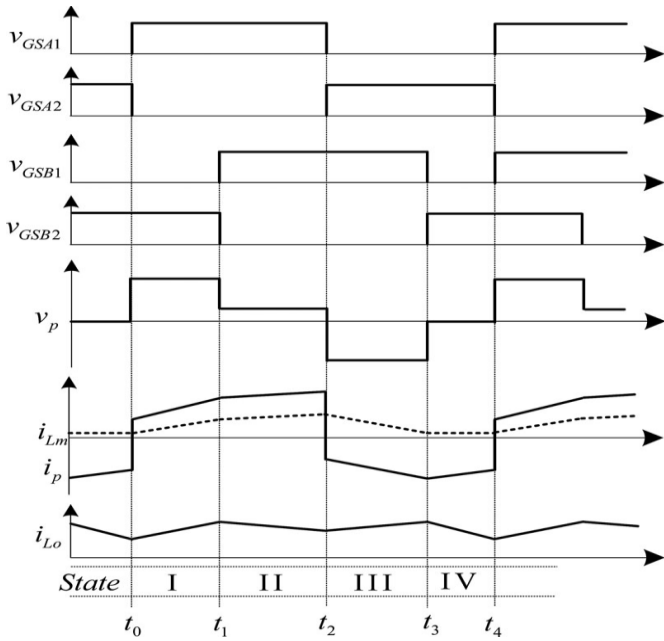


Fig. 6. Key waveforms of the FB-TPC.

State III [t2 –t3]: At t2, SA1 turns OFF and SA2 turns ON. a negative voltage is applied on the primary winding of the transformer [see Fig. 6(c)]

State IV [t3 –t4]: At t3, SB 1 turns OFF and SB 2 turns ON. the voltage across the primary winding is clamped at zero, and i_{Lm} freewheels through SA2 and SB 2 [see Fig. 6(d)]

B. ZVS Analysis

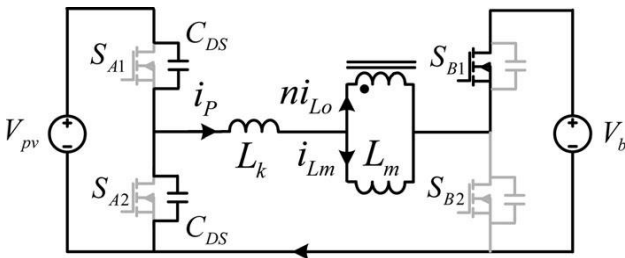


Fig. 7. ZVS analysis of SA2.

According to the analysis, the operation of the FB-TPC is similar to the operation of a phase-shift FBC with the two switches SA1 (SB1) and SA2 (SB2), driven with complementary signals. The proposed FB-TPC can utilize the leakage inductance, filter inductance, and the output capacitors (parasitic drain to source capacitors) of the switches to realize ZVS, zero-voltage turn-on, and zero-voltage turn-off for all the switches. The operation principle is similar to the phase-shift FBC [23], [24]. The only difference is that in the proposed FBTPC, the magnetizing inductor of the transformer L_m can also help to achieve ZVS of the switches if the direction of i_{Lm} is the same as i_p . Take SA2 as an example. As shown in Fig. 7, where only the primary circuit is shown for simplicity, considering the leakage inductance L_k , when SB 1 is ON and SA1 is turned OFF, $i_p = i_{Lm} + ni_{Lo}$, the energy stored in L_k and L_m will release to charge or discharge the parasitic

drain to source capacitors of SA1 and SA2 . As a result, with a proper dead time, ZVS of SA2 can be achieved if the following condition is satisfied

$$\frac{1}{2} [L_k(i_{Lm} + ni_{Lo})^2 + L_m i_{Lm}^2] > C_{DS} V_b^2.$$

C. Design Consideration

As for the semiconductor device stress, the FB-TPC is similar to the traditional FBC. But a key difference between these two converters is that the magnetizing inductance of the transformer L_m is operated as an inductor as well. We also take the $V_{pv} \geq V_b$ case as an example for analysis. From (1), in the steady state, we have

$$V_{pv} I_{pv} = V_b I_b + V_o I_o$$

According to the switching states I and II, we have

$$I_{pv} = DA1 (I_{Lm} + nI_o)$$

Where I_{Lm} is the average magnetizing current of the transformer, and then we have

$$I_{Lm} = I_{pv} / DA1 - nI_o$$

it can be seen that the larger the $DA1$, the smaller the I_{Lm} .

According to the switching states II and III, we have

$$\begin{aligned} I_b &= D2 (I_{Lm} + nI_o) - D3 (I_{Lm} - nI_o) \\ &= (DB1 - 2D3)I_{Lm} + DB1nI_o \end{aligned}$$

Then the average transformer magnetizing current I_{Lm} can also be given by the following equation:

$$I_{Lm} = (I_b - DB1nI_o) / (DB1 - 2D3)$$

$D3$ is determined by V_b and V_o , therefore, the larger the $DB1$ the smaller the I_{Lm} . It is noticed that I_{Lm} can be reduced by increasing the nominal values of $DA1$ and $DB1$; this result is also valid for the $V_{pv} < V_b$ case by following the same analysis procedure. Therefore, the value of I_{Lm} can be decreased with a properly designed modulation scheme.

IV. Simulation, Hardware and System Results

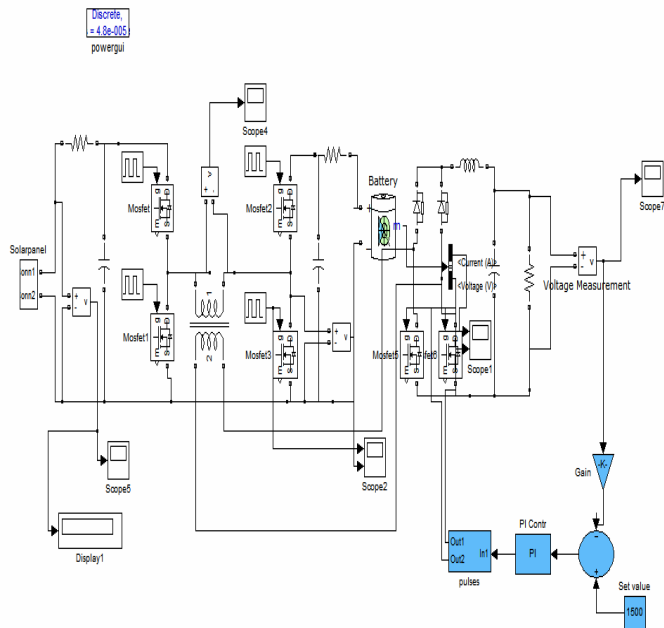


Fig. 8. Simulink model of proposed circuit for R load (closed loop)

In closed loop system, the output will be fed back through the controller to the input. The dc input given to the inductor boost is doubly boost and then given to the resonant cell, which is used to reduce switching losses and diode recovery losses. Then it will given to load, here we are using R load in the closed loop circuit.

The controller used for this circuit is PID circuit. Hence if there is any over distortion or variation in results, the PID controller will given the feedback to input according input varied. It gives better result compared to the open loop R load, because of stable result.

INPUT VOLTAGE

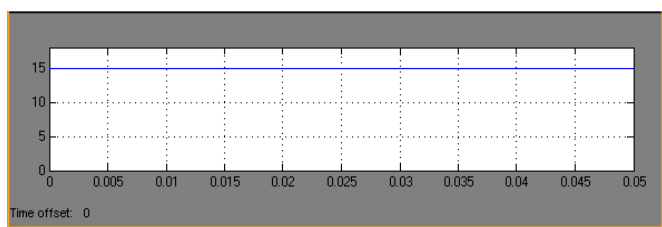


Fig. 9. $V_{in} = 15V$ (Input voltage)

OUTPUT VOLTAGE

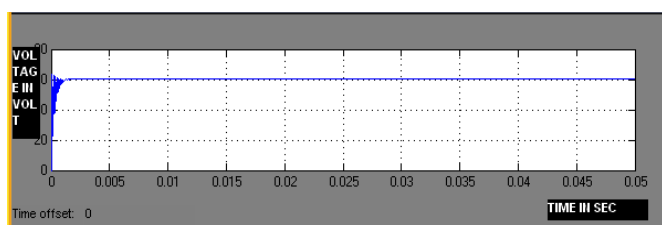


Fig. 10. $V_{out} = 60V$ (Output voltage)

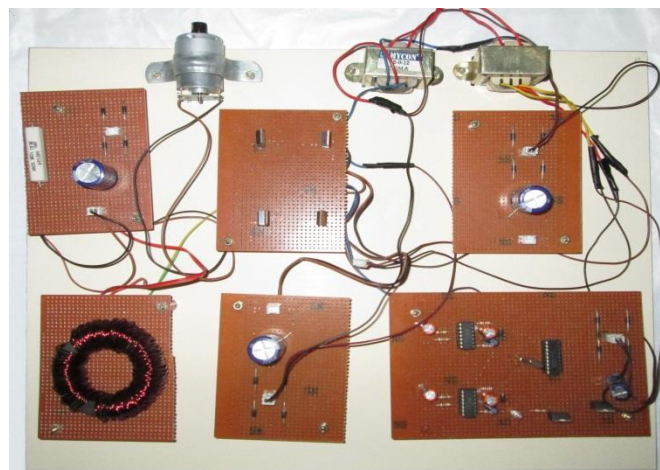


Fig. 11. Picture of the prototype.

COMPARISON OF THE TP-FBC WITH PARALLELED INDUCTOR & TP-FBC

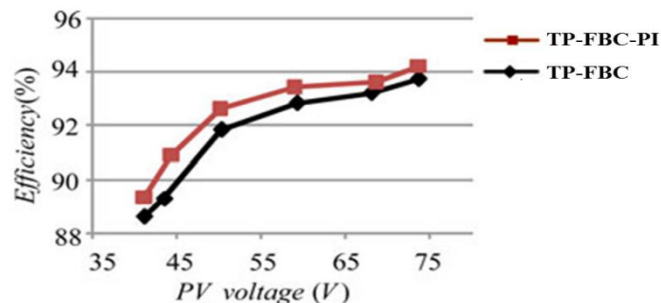


Fig. 12. Efficiency curves, under full power, versus PV source voltage.

V. EXPERIMENTAL RESULTS

An FB-TPC prototype controlled by a TMS320F2808 DSP, as shown in Fig. 10, is built with the key parameters listed in Table II. A variable resistor in series with a dc source is used to simulate the PV characteristics. The steady-state waveforms of the converter with 15V input voltage at full load are shown in Fig. 9. Fig. 13 shows the waveforms under the input mode and Fig. 14 shows the waveforms of the output mode.

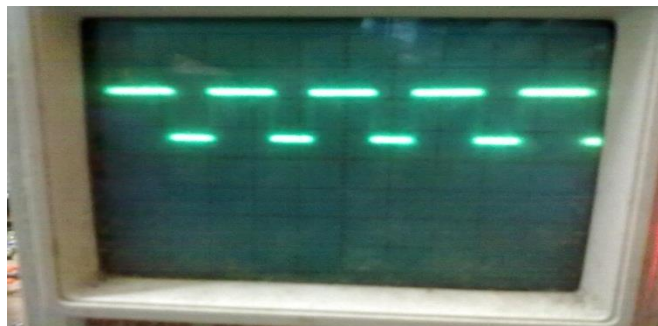


Fig.13. input waveforms of the TP-FBC

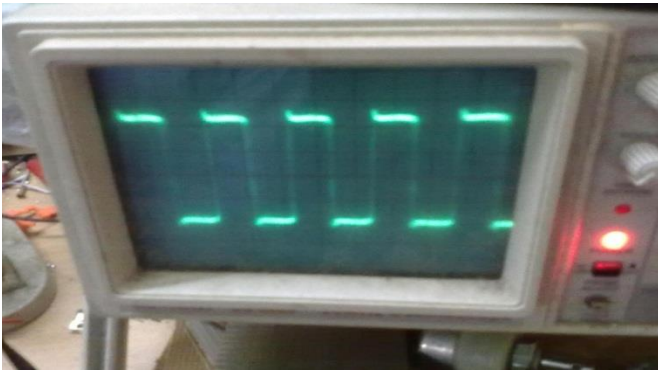


Fig. 14. Output waveforms of the TP-FBC

VII. Improvement of the TP-FBC

The key characteristic of the TP-FBC is that the magnetizing Inductor of the transformer also functions as a filter inductor, and the primary circuit acts as a four-switch buck-boost converter to bridge the power flow between the two ports on the primary side. However, the energy storage ability of the transformer may limit the power rating of the TP-FBC. To overcome this drawback, a block capacitor can be placed in series with the primary winding and another optimally designed inductor placed in parallel with the transformer to transfer power between the primary side's two ports, as shown in Fig. 14. The improved converter, named TP-FBC with a paralleled inductor (TP-FBC-PI), can be seen as a combination of a four-switch buck-boost converter and an FBC with shared power switches. It is suitable for the higher Power application but another inductor is required which may degrade the power density of the converter.

VI. CONCLUSION

A Full-bridge converter implemented with Three-port Full-bridges has been proposed in this paper. A control method has been presented for achieving soft switching over a wide input range. A PWM control method is applied to the Three-port Full-bridge converter. The particular structure of a boost Full-bridge, interfaces the port having a wide operating voltage, makes it possible to handle voltage variations at this port by adjusting the duty cycle of all the three Full-bridges. With this approach, the operation of the converter is optimized with both current stress and rms loss being reduced. Moreover, soft-switching conditions for all switches are achievable over the entire phase shift region. Control scheme based on multiple PI regulators manages the power flow, regulates the output, and adjusts the duty cycle in response to the varying voltage on the port. Simulation and experimental results were presented, validating the effectiveness of the proposed converter and its control scheme.

REFERENCES

- [1] Kwasinski A, "Quantitative evaluation of DC microgrids availability: Effects of system architecture and converter topology design choices," IEEE TRANS. POWER ELECTRON., VOL.26, NO.3, MAR. 2011.
- [2] Jiang W and Fahimi B, "Multi-port power electric interface for renewable energy sources," in Proc. IEEE APPL. POWER ELECTRON. CONF., APRIL. 2009.
- [3] Jiang W and Fahimi B, "Multiport power electronic interface—Concept modeling and design," IEEE TRANS. POWER ELECTRON., VOL.26, NO.7, JUL. 2011.
- [4] Tao H, Duarte J, and Hendrix M, "Multiport converters for hybrid power sources," IEEE PROC. POWER ELECTRON. SPEC. CONF., JUL. 2008.
- [5] TaoH, Kotsopoulos and Hendrix M, "Family of multiport bidirectional dc-dc converters," INST. ELECTR. ENG. PROC. ELECT. POWER APPL., VOL.153, NO.15, MAY 2006.
- [6] Abdel-Rahman, and BatarsehI, "Modeling and control of three-port DC/DC converter interface for satellite applications," IEEE TRANS. POWER ELECTRON, VOL.25, NO.3, MAR.2010.
- [7] Qian Z, and BatarsehI, "An integrated threeport inverter for stand-alone PV applications," presented at THE IEEE ENERGY CONVERS. CONGR. EXPO. ATLANTA, GA, 2010.
- [8] Zhang J, and GeH, "A family of threeport half-bridge converters for a stand-alone renewable power system," IEEE TRANS. POWER ELECTRON., VOL.26, NO.9, SEP. 2011.
- [9] Zhao C, and JohannW, "An isolated three-port bidirectional DC-DC converter with decoupled power flow management," IEEE TRANS. POWER ELECTRON., VOL.23, NO.5, SEP. 2008.
- [10] DuarteL, and SimoesG, "Three-port bidirectional converter for hybrid fuel cell systems," IEEE TRANS. POWER ELECTRON, VOL.22, NO.2, MAR. 2007.
- [11] TaoH, and Marcel M, "Three-port triple-half-bridge bidirectional converter with zero-voltage switching," IEEE TRANS. POWER ELECTRON., VOL.23, NO.2, MAR. 2008.

Acknowledgement:



Mr. M. Ragavendran has received the Bachelor degree in Electrical and Electronics Engineering from Kanchi Pallavan Engineering College, Anna University, India in 2011. He is pursuing Master of Engineering in Power Electronics and Drives from Jeppiaar Engineering College, Anna University, India



Prof. Dr. M.Sasikumar has received the Bachelor degree in Electrical and Electronics Engineering from K.S.Rangasamy College of Technology, Madras University, India in 1999, and the M.Tech degree in power electronics from VIT University, in 2006. He has obtained his Ph.d. degree from Sathyabama University, Chennai. Currently he is working as a Professor

and Head in Jeppiaar Engineering College, Chennai Tamilnadu, India. He has published papers in National, International conferences and journals in the field of power electronics and wind energy conversion systems. His area of interest includes in the fields of wind energy systems and power converter with soft switching PWM schemes. He is a life member of ISTE